Proceedings of Global Power and Propulsion Society
ISSN-Nr: 2504-4400
GPPS Xi'an21
18th – 20th October, 2021
www.gpps.global

GPPS-TC-2021-0076

SURROGATE-BASED AERODYNAMIC SHAPE OPTIMIZATION OF CONTRA ROTATING OPEN ROTOR

Qihang Wang
Northwestern Polytechnical University
jackwang64@outlook.com
Xi'an, Shaanxi, People's Republic of China

Li Zhou
Northwestern Polytechnical University
zhouli@nwpu.edu.cn
Xi'an, Shaanxi, People's Republic of China

Zhanxue Wang
Northwestern Polytechnical University
wangzx@nwpu.edu.cn
Xi'an, Shaanxi, People's Republic of China

ABSTRACT

In this paper, the study on aerodynamic shape optimization of contra rotating open rotor is presented. Computational fluid dynamics simulations combined with Neural networks (radial basis function) surrogate model is applied to solve the problem. The difficulty is associated with both time-consuming computational fluid dynamics simulations and the large number of design variables involved. The contra rotating open rotor optimization problem is to find the variables that produces the maximum propulsive efficiency for a limited range of thrust requirement. The DOE (deign of experiment) process is completed by uniform design and computational fluid dynamics simulations. The non-linear programming by quadratic lagrangian (NLPQL) is used to tackle the optimization problem. Infill sampling criteria is used in this process to reduce demand on the number of initial samples while keep the accuracy of surrogate model. After building the initial surrogate from DOE sampling, the update point is selected according to the infill sampling criteria. It shows that the infill sampling criteria is helpful in surrogate model building process and surrogate-based optimization method is valid for aerodynamic shape optimization of contra rotating open rotor.

INTRODUCTION

With the development of the aviation industry, especially in the field of civil aviation, the next generation of aircraft engines must be more fuel efficient and reduce pollutant emissions. However, due to the limitation of the diameter of nacelle, bypass ratio of the traditional turbofan engine is limited. Thus, the propulsion efficiency of turbofan engine has a upper bound. So traditional turbofan engine has little potential for energy saving and emission reduction, so a new concept aircraft engine is needed.

The contra rotating open rotor is a new concept engine. Compared with the traditional turbofan engine, open rotor engine has no bypass and can be considered as an aircraft engine with very high effective bypass ratio. It is expected to replace the high-speed subsonic military turbofan engine and it has a great potential for commercial applications [1]. Since there is no bypass, it is lighter in weight and it can be shown that an open rotor engine can reduce fuel consumption by 20% to 40% compared to conventional turbofan engines [2]. The flight test taken in Boeing B727 and McDonnell Douglas MD80 flying test beds proves its feasibility [3]. It means that the open rotor engine has no obstacles in terms of technology and installation. The biggest advantage of contra rotating open rotor is its high propulsion efficiency. Thus, the rotors become the most significant components of contra rotating open rotor because the efficiency of the rotor has a great impact on the propulsion efficiency of the engine. So, the aerodynamic optimization of the rotor is very important. Martin et.al applied an improved RANS-lifting-line coupling method to predict the open rotor acronymic performance [4]. Thomas et.al presented a continuous adjoint formulation for rotating Euler equations. The formulation is applied to optimize the blade of open rotor by gradient-based optimization framework [5]. Schnell et.al presented a way to parameterize the

This work is licensed under **Attribution-NonCommercial-NoDerivatives 4.0 International** (CC-BY-NC-ND).
See: https://creativecommons.org/licenses/by-nc-nd/4.0/legalcode

complete contra rotating open rotor geometry. An evolutionary algorithm with metamodel acceleration techniques is applied to optimize the aerodynamic and acoustic performance of contra rotating open rotor [6].

This paper improves the method of samples selection through analysis of coupling relation between front and rear rotors. Compared to the single-row propeller, the simultaneous optimization of the front and rear stages makes the calculation much more complicated. The mutual interference between rotors makes the variables of rear and front rotors couple with each other. Flow state of rear rotor is influenced by the wake flow of front rotor, the wake and tip vortex of front rotor have an impact on the inlet condition of rear rotor. The flow state of front rotor is also influenced by the rear rotor because of potential flow. This kind of influence is weaker than that caused by the wake flow, researches find that the rear rotor has no substantial effect on the position of the front rotor tip vortex [7]. The optimization problem can be better solved if this coupling relation disappear. However, it's impossible to totally remove this coupling relation because of the flow characteristics of contra rotating open rotor. But when it comes to some responses, like efficiency, the coupling relation tends to be inconspicuous.

For the optimization of contra rotating open rotor, there exists many parameters decide the performance of the open rotor. Furthermore, the geometric surface of open rotor tends to be complex because of the sweep and twist of the blades. The requirement of the quantity and quality of grid is extremely high. It will take a lot of computer resources and time to optimize the open rotor with CFD method. The problem of optimization is a typical black-box problem, a set of inputs always corresponds to a set of outputs. To better solve this kind of problem, the surrogate model is employed. Many researchers have done a lot of work on the surrogate-based optimization problem [8-11]. The response surface methodology [12-13] become a research hotspot. Especially, surrogate model is widely applied in the field of Turbomachinery, such as axial compressor [14] and helicopter rotor blade [15]. Gonzalo et.al also performed two independent aerodynamic optimizations of contra rotating open rotor with different blade profiles by radial basis functions coupled with multi-objective differential evolution [16].

In the process of surrogated-based optimization method, quality of the design of experiment (DOE) and the speed of optimization process greatly influences the result of surrogated-based optimization method. Atharv Bhosekar proved the common observation that more sampling points can describe the surrogate model more accurately [17]. However, only increasing the number of sample points is infeasible for the aerodynamic shape optimization problem. With regard to the ideal DOE, the sampling points should be scattered in the domain uniformly and entirety. In addition, the selection of variables should avoid the local optima which may cause the difficulties in the process of optimization.

For problems with many variables, the conventional establishment method of surrogate model is no longer applicable because high-precision surrogate model cannot be built only by initial DOE. Thus, infill sampling criteria is applied to reduce the requirement on the quantity of initial samples, meanwhile, build high-accuracy model. The aim of infilling samples is to accurately describe the area where the optima might exist instead of the whole design domain. Lots of work has been done to find the suitable Infill sampling criteria. J.M.Parr compared the performance of four different infill sampling criteria on two artificial test problem, including single update infill sampling criteria and multiple update sampling criteria [18].Liu jun et.al introduced several infill sampling criteria including, maximizing the constrained expected improvement, minimizing the predicted objective function, minimizing the lower confidence bounding, maximizing the probability of improvement, and maximizing the mean squared error. The aerodynamic optimization results show slight differences among them [19]. The most commonly used infill sampling criteria is minimizing the predicted objective function (MP). The MP can make the surrogate more accurate, however it can also make the optimization fall into the local optima [20]. The infill sampling criteria above is commonly obtained through mathematical deduction.

When it comes to the optimization, traditional methods include genetic algorithm and gradient search. Different optimization methods bring different advantages and disadvantages. Gradient search can rapidly search the optima compared to genetic algorithm [21]. The advantage of genetic algorithm is that the result can cover a complex Pareto-front. When the Pareto-front is not complex, the results of these two methods have negligible contrast.

It is clear that very little literature is available on the surrogate-based aerodynamic shape optimization of contra rotating open rotor. Especially, this paper introduces two infill sampling criteria to reduce the requirement on the quantity of DOE samples. The first one is based on the parameter analysis of contra rotating open rotor. The second one is based on the mathematical principles. The surrogate model in this paper is built by radial basis function neural networks and the optima is searched by NLPQL. The optimization result proves the feasibility and validity of this method.

METHODOLOGY

1 Design of Experiment (DOE)

Before building surrogate model, design of experiment (DOE) should be carefully considerated. During the DOE process, the factors, levels, design matrix are determined. For problem with a great many optimized variables, it is often significant and always computationally beneficial to reduce the number of sampling points. Therefore, an ideal DOE should cover the design domain comprehensively while control the number of sample points within a certain number. Common DOE method includes full factorial design, orthogonal arrays, central composite design, Latin hypercube design, Box-

behnken design, and so forth. This paper selects uniform design to do DOE. Uniform design is a DOE method which seeks the sampling points uniformly scattered on the design domain [22].

The principle of uniform design is similar to that of Latin hypercube design. However, uniform design selects the center of hypercube as the test point. As usual, uniform design use a normalization table to specify sampling points. uniform design table can be written as $U_n(m^k)$, n is the number of experiments, m is the number of levels, k is the number of factors. The uniform table is chosen by the number of factors and levels. For a certain optimization problem, the number of the factors, in other word, the optimized variables, is determined. The only one undetermined parameter of uniform design is the number of levels. There is a contradiction between the number of samples and accuracy of model. The uniform design provides several parameters to check the quality of uniform design table, including centered L2-discrepancy, L2-discrepancy, correction error, symmetry discrepancy, wrap-around discrepancy and so on. The mostly used is centered L2-discrepancy. According to the value of centered L2-discrepancy, the number of levels can be determined. That means the number of sampling points is determined. The smaller the value of L2-discrepancy, the better the uniformity of sampling points. For the six variables selected for the aerodynamic shape optimization of contra rotating open rotor, the number of factors of uniform design must be six. The number of levels can be selected depending on the value of L2-discrepancy.

2 Geometry Parameterization

Because of high flight Mach number, the blades of typical open rotor commonly have large chord length and small thickness. To reduce shock wave resistance, the blade usually has a distinguishing sweep. As common observation, the sweep function varies from negative value at root of blade to positive value up to the tip. The blade used in this paper is a set of standard blades designed by the three-dimensional design, the airfoil used in the three-dimensional design is NACA0016. The camber line is defined by double circular arc. The degree of bending is measured by turning angle of the airfoil. The radius of blades is 2m. The front and rear rotors have different geometric characteristics. The distribution of chord, chamber and thickness is shown in FIGURE 1. The chord, stagger angle and thickness are normalized by maximum chord, stagger angle and thickness. The maximum chord is 1.008m and 1.018m. The maximum stagger angle is 72.264° and 69.388° .The maximum thickness is 0.107m and 0.108m.

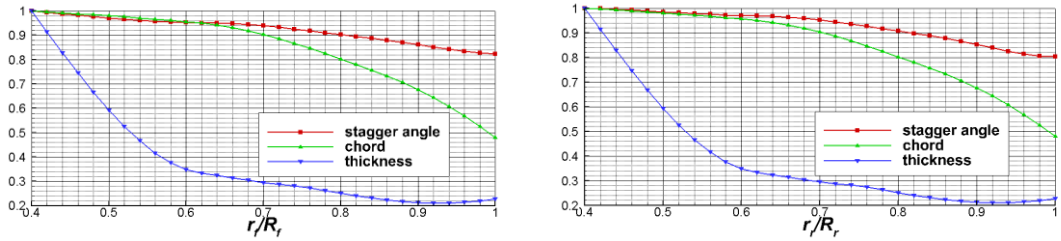

(a) geometric parameters of front rotor (b) geometric parameters of rear rotor

FIGURE 1: Geometric parameters of open rotor

For a given airfoil, chord will influence the load and maximum thickness will decide the degree of boundary layer separation. Those two variables of every two-dimensional section can decide the flowing state of section. These effects accumulate to affect the thrust and efficiency of the whole blade. For the aerodynamic shape optimization of the open rotor blade, the distribution of chord and maximum thickness should be taken as the optimization variables. Because of the requirement that the blade should have an overall change, this paper select the X_{zoom} of front and rear rotor, Y_{zoom} of front and rear rotor, stagger angle β of front and rear rotor as the variables for optimization. Xzoom is defined as the factor of x coordinate value scaling. Yzoom is defined as the factor of y coordinate value scaling. FIGURE 2 shows an example of this scaling process. The Those six variables are dependent of each other, so there will be six independent variables decide the shape of the contra rotating open rotor.

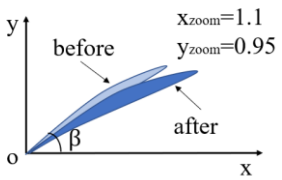

FIGURE 2: Definition of optimization variables

In the process of changing shape, operate scaling first, then rotate the blade the change the stagger angle. After scaling and rotating, the chord, stagger angle and maximum thickness become :

$$\beta' = \arctan\left(\frac{x_{zoom}}{y_{zoom}} \cdot tan\,\beta\right) - \Delta\beta \qquad (1)$$

$$\rho' = \rho \cdot \sqrt{x_{zoom}^2 \cdot (sin\beta)^2 + y_{zoom}^2 \cdot (cos\beta)^2} \qquad (2)$$

$$t' = t \cdot \sqrt{x_{zoom}^2 \cdot (cos\beta)^2 + y_{zoom}^2 \cdot (sin\beta)^2} \qquad (3)$$

In the above formula, β is stagger angle, ρ is chord and t is maximum thickness .For a certain flight condition shown in TABLE 1, the X_{zoom} of both front and rear rotors are 1.2.and Y_{zoom} of both front and rear rotors are 0.8. The stagger angle change $\Delta\beta$ is -9. The spacing between front and rear rotor is 1.6m.

TABLE 1: Design parameters

	Parameter	Unit	Value
Flight condition	Flight altitude	m	10668
	Mach number		0.785
Front rotor	Number of blades		8
	Rotation speed	rpm	1100
	Tip diameter	m	4
	Hub diameter	m	1.6
Rear rotor	Number of blades		8
	Rotation speed	rpm	-1100
	Tip diameter	m	4
	Hub diameter	m	1.6
	Rotor spacing	m	1.6

This geometry is taken as the objectives to be optimized. In order to simplify the difficulty of numerical simulation, the complex hub shape is not considered, and the hub is considered to be an infinite cylinder. The hub ratio of this contra rotating open rotor is 0.4. The baseline geometry of this open rotor is shown in FIGURE 3.

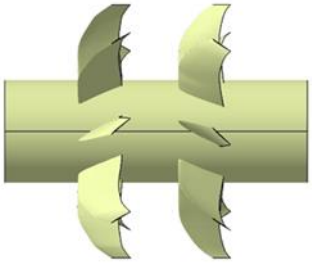

FIGURE 3: Geometry of baseline contra rotating open rotor

3 Computational Fluid Dynamics (CFD)

The Reynolds averaged Navier-Stokes(RANS) equations were solved by finite volume method using second-order upwind format. The (k-ε) turbulence model was employed to close the RANS equations. The geometry is put into a cylindrical coordinate system. To decrease the quantity of grids, calculation was carried on in a single flow channel of contra rotating open rotor (One eighth cylinder). Because the blades of contra rotating open rotor have significant outflow characteristics, the length and radius of the far field must be large enough. Compared with blade rotation domain, grid density in far field do not need to be large. So, internal and external nested grid topology is selected to generate mesh. The whole computing domain is divided into internal domain and external domain. Internal domain contains the front and rear rotors. The radius of internal domain is 1.5 times the blade radius. The length of internal domain is 3 times the front and rear rotors spacing. External domain is the far field. The grid at the interface with the internal domain is densified. The radius of external domain is 7.5 times the blade radius. The length of external domain is 20 times the front and rear rotors spacing. Because this open rotor has contra rotating characteristics, the internal domain is divided into two rotation domains with opposite rotation speed. The mesh and boundary condition are shown in figure 3.

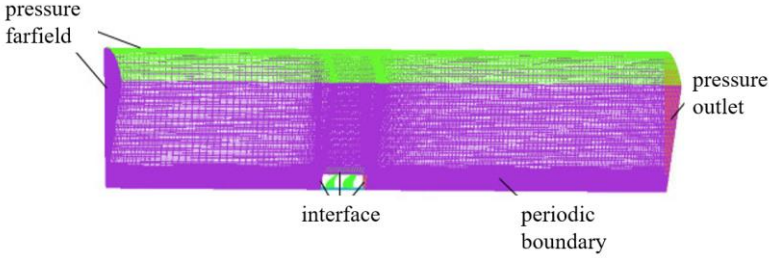

FIGURE 4: Boundary condition

In order to verify the numerical simulation method, the numerical simulation results are compared and verified by using the test data in NASA report. In order to ensure the numerical verification under the same boundary conditions, the

installation angle of the front and rear rotors are 58.5° and 55.7° , and the working state is cruise. The results of numerical calculation under the same boundary conditions are compared with the test data, as shown in FIGURE 2. It can be seen that the calculated values are basically consistent with the test values, and the maximum error occurs when the advance ratio J = 2.68, The error is 3.26%, which meets the error requirements, which verifies the rationality of the numerical simulation method adopted in this paper.

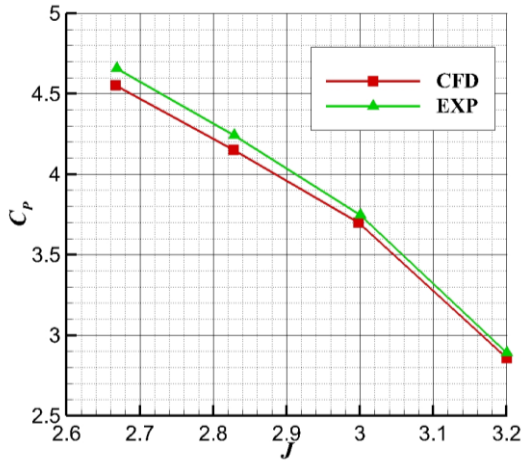

FIGURE 5: Comparison and verification result of power coefficient

In order to eliminate the influence of grid on the CFD results, the grid independency is checked, as shown in TABLE 2:

TABLE 2: Grid independency

number of cells	1,087,780	1,944,461	4,028,746
η	0.8027	0.8047	0.8055
T	25840.66	26044.23	26190.73
$\Delta\%$		0.25%	0.10%
$\Delta\%$		0.79%	0.56%

It can be found that efficiency calculated by 2 million cells is similar to that by 1 million cells and 4 million cells. The thrust calculated by 2 million cells has a smaller difference with 4 million than 1 million. For the sake of saving computing resources, grid with 2 million cells is taken as the CFD grid.

4 Establishment of Surrogate Model and Optimization

Radial basis function (RBF) is a set of basis functions with radial distance as variable. Radial basis function Neural network is a three-layer feedforward neural network composed of input layer, hidden layer and output layer. In radial basis function Neural network, the local response function of hidden layer is radial basis function. Output layer provides responses. The RBF Neural network applied in this paper select Gaussian-RBF as the hidden layer. Gaussian-RBF is a kind of probability distribution function. Transformation from input layer to hidden layer is nonlinear. The purpose of this transformation is to map the input variables from the low-dimensional space to the high-dimensional space of the hidden layer. In this paper, the Radial basis function Neural network is built by *ISIGHT*.

NLPQL (Non-Linear Programming by Quadratic Lagrangian) is applied in this paper to carry on the optimization. NLPQL is typical gradient-based optimization method which has proved to be both efficient and effective in dealing with optimization problem. Essentially, NLPQL is a sequential quadratic programming (SQP) method. The principle of this kind of methods is to expand the objective function with the second order Taylor series. Then linearize constraints and solve one or several quadratic programming subproblems to find next iteration value. The key process of SQP is find the quadratic programming subproblem. NLPQL uses a matrix B_k,which is similar to the Newton matrix, to define second order approximation of Lagrangian function $L(x,u)$ and $L(x_k,\ u_k)$ similar to Hessian matrix. By this way, quadratic programming subproblem is got. In order to achieve global convergence of NLPQL algorithm, additional linear search is applied in NLPQL. Only when the next iteration direction calculated by quadratic programming subproblem is downward, the next step of new iteration will be executed.

5 Infill Sampling Criteria

For the open rotor to be optimized, the six optimization variables can be divided into two categories, one belongs to front rotor, another belongs to the rear rotor. The responses, like thrust and efficiency, of front rotor and rear rotors have a similar changing trend when the variables changes. In other words, change regularity of front and rear rotors' responses are similar. The efficiency and thrust of contra rotating open rotor is the sum of front and rear rotors' thrust and efficiency. So, the surrogate model may have a large gradient area.To accurately describe this surrogate model, especially the high-gradient area, increase the quantity of the sampling points is necessary. So, the infill sampling criteria is essential. This paper introduces two infill sampling criteria to increase the samples, meanwhile, decrease the computational cost of this high-

fidelity numerical simulation. One is based on the flow characteristics of contra rotating open rotor. Another is based on the mathematical approach.

5.1 First infill sampling criteria

The first infill sampling criteria is based on the research on the analysis of coupling relation between contra rotating open rotor's front and rear rotors. For contra rotating open rotor, the front and rear rotors have complex interaction on each other. On the one hand the induced velocity caused by front rotor will influence the rear rotor's inlet condition and so does the rear rotor, on the other hand the flow condition of front rotor will have impact on that of rear rotor because of wake flow. The rear rotor's flow condition also influences the front rotor's flow condition due to the potential flow. The existence of coupling relation between the front and rear rotors makes the optimization problem difficult, however the coupling relation takes a different form in the responses including thrust and efficiency. By the research on the influence of different stagger angle on contra rotating open rotor, it can be found that the coupling relation shows great impact on thrust, while little impact on efficiency.

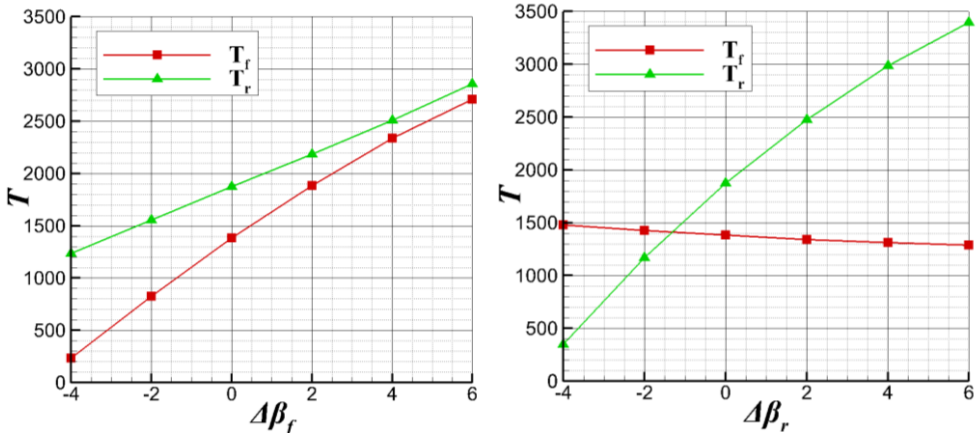

(a) stagger angle of front rotor changes (b) stagger angle of rear rotor changes

FIGURE 6: Compraration of thrust with different stagger angle change

When the stagger angle of front rotors changes, the thrust of both front and rear rotors changes apparently. When the stagger angle of rear rotor changes, the significant variations of front and rear rotors' thrust also exist. The tendency illustrated in FIGURE 6. When it comes to the efficiency, the coupling relation isn't apparent any more. When the stagger angle of front rotor changes, the efficiency of front rotor changes while the efficiency of rear rotor slightly changes. When the stagger angle of rear rotor changes, the efficiency of rear rotor changes while the efficiency of front rotor almost remains unchanged. The tendency illustrated in FIGURE 7.

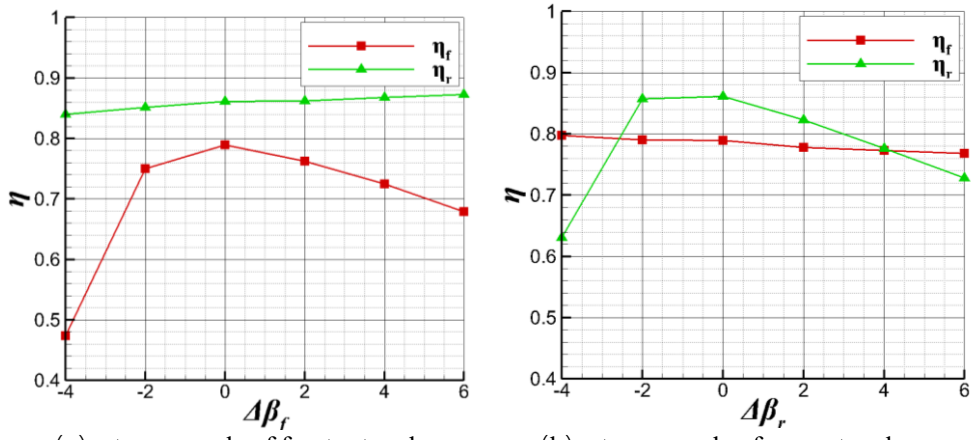

(a) stagger angle of front rotor changes (b) stagger angle of rear rotor changes

FIGURE 7: Compraration of efficiency with different stagger angle change

According to the FIGURE 7(a), the efficiency of front rotor first increases then decreases when the stagger angle increases. This trend is the same as that of cascade channel's flow. When the stagger angle increases, the angle of attack goes through from negative to positive. At beginning, there exists flow separation on the suction surface, the decrease of angle of attack depresses the separation on the suction surface, thus improve the efficiency. As the angle of attack increases further, the separation occurs on the pressure surface, the efficiency decreases. However, the solidity of blades is small, so the flow has obvious outflow characteristics, the restriction ability of blade to flow is weak. Therefore, the change of twist angle caused by the change of stagger angle is small. Moreover, there is a much larger rotor spacing between the front and rear rotors than that between the compressor stages. This big rotor spacing plays an intensive flow straightening role with

regard to the air flow. Above reasons have eventually led to a smaller change of angle of attack of rear rotor than that of front rotor. As long as there is no serious separation in the front rotor, the effect of the front rotor's wake flow on the efficiency of the rear rotor is extremely limited.

When it comes to the rear rotor. The trend is similar to the front rotor. The efficiency of rear rotor first increases then decreases when the stagger angle increases and the efficiency of front rotor nearly keep the same. The front rotor is only affected by rear rotor's potential flow. The change of rear rotor's stagger angle nearly has no influence on that of front rotor. From FIGURE 6(b), it can be found that the thrust of front rotor only has a slight decrease when the stagger angle of rear rotor increase. The decrease can be attributed to the blocking effect caused by the increase of rear rotor's stagger angle. In this process, the efficiency of front rotor remains unchanged.

Through the analysis of this parametric analysis, it can be summarized that contra rotating open rotor has significant outflow characteristics. In addition, contra rotating open rotor has a bigger rotor spacing. Therefore, compared with compressor, the front and rear rotors of contra rotating open rotor has a much more weaker coupling relation. The efficiency of front and rear rotor can be considered to be independent. As for the thrust, the front and rear rotors' are not independent. Because when the thrust of front rotor increases which is due to the increase of front rotor stagger angle, the flowrate will get bigger. The bigger flowrate combined with the bigger stagger angle of rear rotor make the thrust of rear rotor increase. So, the coupling relation in front and rear rotors' thrust still exist and cannot be ignored.

Because of the coupling relation in front and rear rotors' thrust, the rear and front rotors still need to be optimized simultaneously. But the independence of front and rear rotors' efficiency provides an infill sampling criteria. The infilling sample points can be the mixture of the initial DOE's samples. First, the front rotors are sorted according to the efficiency. Second, the rear rotors are sorted according to the efficiency. At last, combine those front rotors and rear rotors with high efficiency to form the new samples. According to this infill sampling criteria, the new samples should have an efficient front rotor and an efficient rear rotor. So, the new samples will have a high efficiency value. In this way, the region of surrogate model with high gradient can be described more accurate.

5.2 Second Infill Sampling Criteria (MP)

Minimizing the predicted objective function (MP) is the simplest and most direct infill sampling criteria. At beginning, the surrogate model built based on the initial DOE samples is assumed to be globally accurate. Then the optima can be searched by the optimization method. The optima found in current surrogate model requires to be test by numerical simulation. If there exist difference between result from CFD and optima optimized according to the surrogate model. The result from CFD will be taken as a new sampling point. This process will continue until converge. The weakness of MP is that the MP may fall into the local optima. The initial value and characteristic of surrogate are important for this infill sampling criteria. But in this paper, the local optima problem is not serious. Because of the first infill sampling criteria, the initial value will really be close to the true optima. Besides, the superposition mode selected is forward superposition. So, the area where true optima exists has a positive monotonicity. As a result, using MP infill sampling criteria can effectively increase the accuracy of the high-gradient area of surrogate model and be helpful to find the optima.

RESULTS AND DISCUSSION

In order to determine the number of the levels in DOE process, the uniform design tables with different number of levels are calculated. The quality of these uniform design tables is shown in TABLE 3. The main decisive parameter is L2-discrepancy. It can be found that when the number of levels increases, the L2-discrepancy decreases constantly. The quality difference between 18 and 20 is bigger than that between 20 and 22. When the number of levels continue to increase, the quality of uniform design table has a slower growth. So, 20 is selected as the number of levels.

TABLE 3: Quality of uniform design tables with different number of levels

number of levels	16	18	20	22	24
Centered L2-discrepancy	0.1595	0.1458	0.1345	0.1259	0.1174
L2-discrepancy	0.0241	0.0217	0.0185	0.0181	0.0176
Correction error	0.2465	0.2253	0.2043	0.1911	0.1799
Symmetry discrepancy	1.4094	1.3040	1.2220	1.1526	1.0979
wrap-around discrepancy	0.3171	0.2952	0.2767	0.2556	0.2391
Condition number	1.4034	1.3115	1.3501	1.2100	1.2053

After choosing the number of levels, the uniform design table is determined. The range of design variables is shown in TABLE4.

TABLE 4: range of design variables

variables	front rotor			rear rotor		
	Xzoom	Yzoom	stagger angle	Xzoom	Yzoom	stagger angle

upper bound	1.25	0.95	-7	1.25	0.95	-7
baseline	1.2	0.8	-9	1.2	0.8	-9
lower bound	1.15	0.65	-11	1.15	0.65	-11

Using numerical simulation, twenty samples are obtained. According to the first infill sampling criteria. The samples with high front rotor efficiency and rear rotor are selected separately. Then, the high-efficiency front rotors and high-efficiency rear rotors are combined randomly. The new samples then carry on numerical simulation. In this way, four infilling samples are obtained. Those twenty-four samples are used to build the initial surrogate model.

The second infill sampling criteria is applied in the optimization process. After three rounds infilling, the final result is obtained. The final optimization results are shown in TABLE 5. The quality of final surrogate model is checked by cross validation. The results are shown in TABLE 6.

TABLE 5: Optimization result

	η_f	η_r	η	T
baseline	0.7660	0.8377	0.8047	26044.2296
optimum	0.7898	0.8612	0.8294	26128.2040
Δ%	3.11%	2.81%	3.07%	0.32%

TABLE 6: Error analysis

Responses	Average error	Maximum	Root mean square	R-Squared
Efficience	0.01718	0.10701	0.0349	0.98915
Thrust	0.02718	0.12092	0.04324	0.9849

The propulsive efficiency increases by 3.07% compared to initial design in the case of 0.322% increase of thrust. The propulsive efficiency of front rotor increases by 3.11%. The propulsive efficiency of rear rotor increases by 2.81%. The changes of chord and stagger angle are shown in FIGURE 8 and FIGURE 9. It can be found that the stagger angle of front and rear rotors increases, meanwhile, the chord length increases as well.

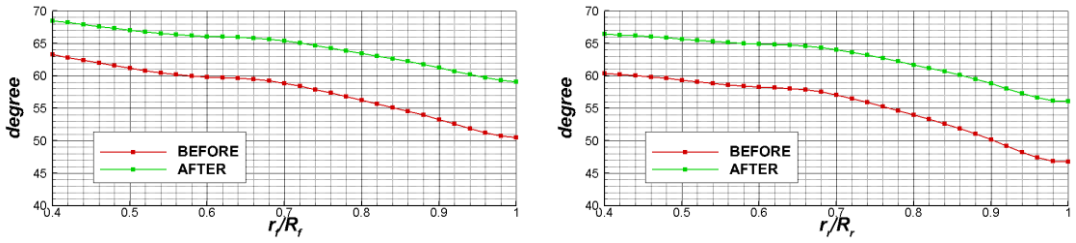

(a) stagger angle of front rotor (b)stagger angle of rear rotor

FIGURE 8: Comparison of stagger angle befor and after optimization

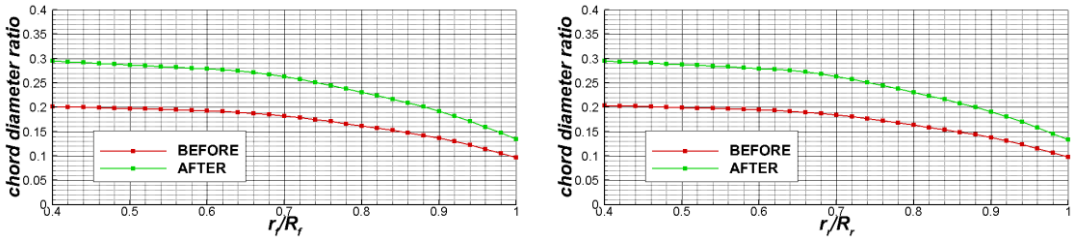

(a) chord of front rotor (b) chord of rear rotor

FIGURE 9: Comparison of thickness befor and after optimization

The static pressure contours of baseline and optimum at 50% blade span are shown in FIGURE 6. It can be found that the shock wave of optimum is weaker than that of baseline. This also explains the reasons for the improvement of efficiency

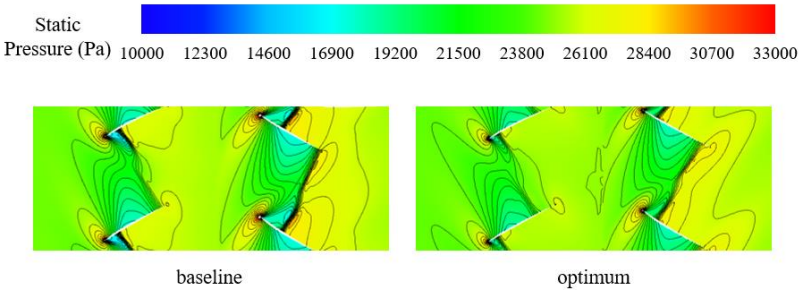

FIGURE 10: Static pressure contours of baseline and optimum at 50% blade span

CONCLUSIONS

This paper presents a method of aerodynamic shape optimization of contra rotating open rotor. The Neural networks (radial basis function) is used to build the surrogate model. The optimization results show the efficiency can be improved by 3.07%. Meanwhile, the thrust almost keep the same to meet the requirement of thrust.

Two infill sampling criteria is introduced in this paper. According to the characteristics of contra rotating open rotor, the most significant one used in building surrogate model is obtained by the analysis of coupling relation of front and rear rotors. Those infilling samples are used to describe the peak area. The efficiency of infilling samples is high enough to describe the peak area of surrogate model.

The contra rotating open rotor has obvious outflow characteristics. The coupling relation between front and rear rotors shows little influence on the efficiency but strongly on the thrust of front and rear rotors. This feature is good for aerodynamic optimization of contra rotating open rotor.

NOMENCLATURE

DOE	deign of experiment
NLPQL	non-linear programming by quadratic lagrangian
RBF	radial basis function
SQP	sequential quadratic programming
MP	minimizing the predicted objective function
X_{zoom}	axial zoom factor
Y_{zoom}	circumferential zoom factor
T	thrust, N
η	efficiency
U	uniform design table
N	sampling point
β	stagger angle
ρ	chord
J	advance ratio
C_P	power coefficient
Subscript:	
f	front rotor
r	rear rotor

ACKNOWLEDGMENTS

The authors would like to express their gratitude for the financial support of the National Natural Science Foundation of China (Nos. 51876176 and 51576163) and MIIT of China.

REFERENCES

[1] A.R.Stuart, Evendale, 1985, "The unducted fan engine," *21th AIAA/SAE/ASME/ASEE Joint Propulsion Conference, Monterey California*, AIAA paper 85-1190, July

[2] Nichols H.E., 1988, "UDF engine/MD80 flight test program," *24th AIAA/SAE/ASME/ASEE Joint Propulsion Conference, Boston (MA, USA)*, AIAA paper 88-2805 July

[3] Cartyle Reid, Cincinnati, 1988, "Overview of flight testing of GE aircraft engines UDF engine," *24th AIAA/SAE/ASME/ASEE Joint Propulsion Conference*, Boston (MA, USA), AIAA paper 88-3082 July

[4] Barry, Martin. 2013, "Open-Rotor Aerodynamics Installation Effects By a RANS-Lifting Line Coupling Method," *AIAA/ASME/SAE/ASEE Joint Propulsion Conference.*

[5] Palacios, Francisco, T. D. Economon , and J. J. Alonso , 2012, "Optimal Shape Design for Open Rotor Blades," *30th AIAA Applied Aerodynamics Conference*.

[6] Schnell R, Yin J, Voss C, et al., 2012, “Assessment and optimization of the aerodynamic and acoustic characteristics of a counter rotating open rotor,” *Journal of Turbomachinery,* 134(6) pp. 061016.

[7] Slaboch P E, Stephens D B, Van Zante D E, et al., 2017, “Effect of Aft Rotor on the Inter-Rotor Flow of an Open Rotor Propulsion System,” *Journal of Engineering for Gas Turbines and Power,* 139(4) pp. 041202.

[8] Booker A J, Dennis J E, Frank P D, et al., 1999, “A rigorous framework for optimization of expensive functions by surrogates,” *Structural optimization,* 17(1) pp. 1-13.

[9] Viana F A C, Haftka R T, Watson L T., 2013, “Efficient global optimization algorithm assisted by multiple surrogate techniques,” *Journal of Global Optimization,* 56(2) pp.669-689.

[10] Jones D R, Schonlau M, Welch W J. ,1998, “Efficient global optimization of expensive black-box functions,” *Journal of Global optimization,* 13(4) pp. 455-492.

[11] Simpson T W, Allen J K, Mistree F. ,1998, “Spatial correlation metamodels for global approximation in structural design optimization,” *Proceedings of ASME 1998 Design Engineering Technical Conferences*. pp. 13-16.

[12] Jones D R. ,2001, “A taxonomy of global optimization methods based on response surfaces,” *Journal of global optimization,* 21(4) pp. 345-383.

[13] Namura N, Shimoyama K, Jeong S, et al. ,2012, “Kriging/RBF-hybrid response surface methodology for highly nonlinear functions,” *Journal of Computational Science and Technology,* 6(3) pp. 81-96.

[14] Samad A, Kim K Y, Goel T, et al. ,2008, “Multiple surrogate modeling for axial compressor blade shape optimization,” *Journal of Propulsion and Power,* 24(2) pp. 301-310.

[15] Glaz B, Goel T, Liu L, et al. ,2009, “Multiple-surrogate approach to helicopter rotor blade vibration reduction,” *AAA Journal,* 47(1) pp. 271-282.

[16] Montero Villar G, Lindblad D, Andersson N., 2019, “Effect of Airfoil Parametrization on the Optimization of Counter Rotating Open Rotors,” *AIAA Scitech 2019 Forum*. pp. 0698.

[17] Bhosekar A, Ierapetritou M., 2018, “Advances in surrogate based modeling, feasibility analysis, and optimization: A review,” *Computers & Chemical Engineering,* 108 pp. 250-267.

[18] Parr J M, Keane A J, Forrester A I J, et al., 2012, “Infill sampling criteria for surrogate-based optimization with constraint handling,” *Engineering Optimization,* 44(10) pp. 1147-1166.

[19] Liu J, Han Z H, Song W P., 2012, “Comparison of infill sampling criteria in kriging-based aerodynamic optimization,” *28th Congress of the International Council of the Aeronautical Sciences*. pp. 23-28.

[20] Forrester A I J, Keane A J., 2009, “Recent advances in surrogate-based optimization,” *Progress in Aerospace Sciences,* 45(1) pp.50-79.

[21] Navid A, Khalilarya S, Taghavifar H., 2016, “Comparing multi-objective non-evolutionary NLPQL and evolutionary genetic algorithm optimization of a DI diesel engine: DoE estimation and creating surrogate model,” *Energy Conversion and Management,* 126 pp. 385-399.

[22] Fang, K. T., Lin, D. K. J., Winker, P., & Zhang, Y. ,2000, “Uniform design: theory and application,” *Technometrics,* 42(3), pp. 237-248.